



Identification of adhesion-associated extracellular matrix component thrombospondin 3 as a prognostic signature for clear cell renal cell carcinoma

Xiangling Chen^{1,2,3,*} , Jiatian Lin^{4,*} , Min Chen⁵ , Qiaoling Chen⁶ , Zhiming Cai¹ , Aifa Tang^{1,2} 

¹Guangdong Provincial Key Laboratory of Systems Biology and Synthetic Biology for Urogenital Tumors, Department of Urology, The First Affiliated Hospital of Shenzhen University, Shenzhen Second People's Hospital, Shenzhen Institute of Translational Medicine, Shenzhen, ²Shenzhen Key Laboratory of Genitourinary Tumor, Department of Urology, The First Affiliated Hospital of Shenzhen University, Shenzhen Second People's Hospital, Shenzhen Institute of Translational Medicine, Shenzhen, ³Shenzhen Institutes of Advanced Technology, Chinese Academy of Sciences, Shenzhen, ⁴Department of Minimally Invasive Intervention, Peking University Shenzhen Hospital, Shenzhen, ⁵State Key Laboratory of Cell Biology, CAS Key Laboratory of Systems Biology, CAS Center for Excellence in Molecular Cell Science, Innovation Center for Cell Signaling Network, Shanghai Institute of Biochemistry and Cell Biology, University of Chinese Academy of Sciences, Shanghai, ⁶Department of Biology, NO.6 Middle School of Changsha, Changsha, China

Purpose: Clear cell renal cell carcinoma (ccRCC) is a highly aggressive disease, and approximately 30% of patients are diagnosed at the metastatic stage. Even with targeted therapies, the prognosis of advanced ccRCC is poor. The aim of this study was to investigate clinical prognosis signatures by analyzing the ccRCC datasets in The Cancer Genome Atlas (TCGA) and the Clinical Proteomic Tumor Analysis Consortium (CPTAC) and the function of thrombospondin 3 (*THBS3*) in ccRCC.

Materials and Methods: We analyzed the ccRCC datasets in TCGA and CPTAC to search for extracellular matrix (ECM)-related and adhesion-associated genes, and conducted overall survival, Cox, and receiver operating characteristic analyses. We also performed CCK8, colony formation, and transwell assays to compare the proliferation and migration ability of *THBS3* knockout cells with those of cells without *THBS3* knockout.

Results: Comprehensive bioinformatics analysis revealed that *THBS3* is a novel candidate oncogene that is overexpressed in ccRCC tumor tissue and that its elevated expression indicates poor prognosis. Our study also showed that knockdown of *THBS3* inhibits proliferation, colony formation, and migration of ccRCC cells.

Conclusions: In summary, our data have revealed that *THBS3* is upregulated in cancer tissues and could be used as a novel prognostic marker for ccRCC. Our findings thus offer theoretical support with bioinformatics analyses to the study of ECM and adhesion proteins in ccRCC, which may provide a new perspective for the clinical management of ccRCC.

Keywords: Clear cell renal cell carcinoma; Human; Metastasis; Thrombospondin 3 protein

This is an Open Access article distributed under the terms of the Creative Commons Attribution Non-Commercial License (<http://creativecommons.org/licenses/by-nc/4.0>) which permits unrestricted non-commercial use, distribution, and reproduction in any medium, provided the original work is properly cited.

Received: 15 July, 2021 • **Revised:** 14 September, 2021 • **Accepted:** 30 September, 2021 • **Published online:** 21 December, 2021

Corresponding Author: Aifa Tang  <https://orcid.org/0000-0002-7516-0506>

Guangdong Provincial Key Laboratory of Systems Biology and Synthetic Biology for Urogenital Tumors, Department of Urology, The First Affiliated Hospital of Shenzhen University, Shenzhen Second People's Hospital, Shenzhen Institute of Translational Medicine, No. 3002 Sungang Xi Road, Futian District, Shenzhen, Guangdong, 518035, China

TEL: +86-755-8300-3435, FAX: +86-0755-82294969, E-mail: tangaifa2018@email.szu.edu.cn

*These authors contributed equally to this study and should be considered co-first authors.

INTRODUCTION

Renal cell carcinoma (RCC), which originates from the renal epithelium, accounts for 90% of cancers in the kidney [1]. Clear cell RCC (ccRCC) is the most common subtype, representing approximately 75% of all cases of renal cancers, and contributes to the majority of cancer-associated deaths [2]. Surgical resection is the main treatment strategy for the management of localized RCC, but approximately 30% of patients experience local recurrence or distant metastasis, and the 5-year survival rate is poor [3,4]. ccRCC is considered resistant to conventional chemotherapy and radiotherapy owing to its complex molecular mechanisms [5]. Hence, it is imperative to explore the molecular mechanisms underlying ccRCC pathogenesis to uncover reliable signatures that could be used as diagnostic biomarkers and therapeutic targets. Accordingly, our study aimed to identify robust molecular signatures with potential to affect the prognosis of ccRCC. We believe that our findings would be supportive for developing novel gene- or protein-targeted drugs for better management of ccRCC.

Poorly defined tumor phenotypes are closely correlated with ccRCC prognosis. Therefore, it is reasonable to screen for factors associated with ccRCC prognosis by identifying tumor phenotype-associated genes or proteins. Recently, several studies have investigated the tumor biomarkers associated with ccRCC metastasis, such as the oncogenic driver *SEMBT1* [6] and the dopamine transporter *SLC6A3* [7]. In addition, some studies have used gene expression profile data generated by high-throughput platforms to explore ccRCC gene signatures and identify genes such as *AHNAK2* [8]. However, the research focusing on genes that can predict the metastasis of ccRCC is still limited. In this study, we aimed to screen ccRCC tumor phenotype-associated differentially expressed genes and proteins (DEGs and DEPs, respectively) in both The Cancer Genome Atlas (TCGA) and the Clinical Proteomic Tumor Analysis Consortium (CPTAC). We screened a total of 127 extracellular matrix (ECM) and adhesion-associated genes or proteins that regulate tissue development, homeostasis, cell growth, differentiation, and migration [9,10] for further analyses.

Thrombospondin 3 (*THBS3*) was originally discovered during sequencing of DNA upstream from the transcription start site of the mouse *Mucl* (episialin) gene [11], which is a member of the *THBS* family. Thrombospondins are secreted ECM proteins, of which there are five homologous members. They share a complex domain structure and have numerous binding partners in the ECM and multiple cell surface receptors [12]. *THBS3* functions in heart [13], skin [14], and bone

development [15]. However, limited knowledge exists about the role of *THBS3* during disease conditions, especially in tumors. *THBS3* has been reported to stimulate osteosarcoma [16]. In addition, *THBS3* demonstrates the greatest mRNA abundance in the kidney, pituitary gland, trachea, uterus, and fetal kidney [17]. These findings suggest that *THBS3* may play an important role in disease progression, especially in kidney-associated diseases. The clinical significance and prognostic value of *THBS3* in ccRCC patients remain largely unknown and therefore warrant further systematic investigation.

MATERIALS AND METHODS

1. Cell culture

ACHN and 769-P cells were purchased from the Cell Bank of the Chinese Academy of Sciences (Shanghai, China). 769-P cells were cultured in RPMI 1640 (Gibco, Beijing, China) and ACHN cells in MEM (Gibco) with 10% fetal bovine serum (FBS) and 1% penicillin/streptomycin in an incubator at 37°C with 5% CO₂.

2. siRNA transfection

siRNA sequences were synthesized by GenePharma (Shanghai, China). The two siRNAs of *THBS3* were as follows: 5'-CCAGATTCAGAATTCAGAATT-3' (si*THBS3*-1), 5'-CAATCAGAAGGACTCAGATTT-3' (si*THBS3*-2). All siRNAs were transfected at a final concentration of 60 nM with Lipofectamine 3000 (L3000-015; Thermo Fisher, Invitrogen, Carlsbad, CA, USA).

3. CCK8 cell proliferation assay

After 24 hours of targeted siRNA transfection, cells were seeded into 96-well plates (3,000 cells/well, 4 replicate wells per group). The Cell Counting Kit 8 (CK04; Dojindo, Kumamoto Prefecture, Japan) was used according to the manufacturer's instructions. We used a microplate reader to detect the optical density at 450 nm.

4. Colony formation assay

After 24 hours of targeted siRNA transfection, cells were seeded and cultured in 6-well plates (1,500 cells/well) for 14 days. Each well was then washed with phosphate buffer saline (PBS) two times, and the cells were fixed with methanol for 15 minutes and stained with 0.5% crystal violet solution for 20 minutes. The numbers of colonies per well were manually counted.

5. 5-Ethynyl-2'-deoxyuridine incorporation assay

5-Ethynyl-2'-deoxyuridine (EDU) testing was based on previous reports [18]. After 24 hours of targeted siRNA transfection, cells were seeded into 96-well plates, incubated with 50 μM EDU for 2 hours, and stained with Apollo fluorescent dye (Cell-Light EDU Apollo567 In Vitro Kit, C10310-1; Ribobio, Guangzhou, China). Images were acquired under a fluorescent microscope.

6. Transwell migration assay

The cell migration assay was conducted using a transwell chamber (3422, 8-μm pore size; Corning company, Corning, NY, USA). After 24 hours of targeted siRNA transfection, cells were placed on the upper layer with no FBS media and lower chamber with media containing 20% FBS. Cells were incubated for 24 hours, fixed with 4% paraformaldehyde, dried, and stained with 0.1% crystal violet, and the upper chamber cells were gently removed. Cells that had passed through the pore and adhered to the lower membrane surface were counted manually.

7. Wound-healing assays

Cells were cultured in 12-well plates for wound-healing

assays. After 72 hours of targeted siRNA transfection, the cell density reached 100%, and the scratch operation was carried out. The plates were photographed at 0 and 10 hours after the scratch operation. The wound edges were indicated by black lines. The percentage of wound closure was calculated.

8. RNA isolation and quantitative real-time PCR (RT-PCR)

Total RNA was isolated from cells using Trizol reagent (Thermo fisher, Ambion by Life technologies, Carlsbad, CA, USA). Isolated total RNA was reverse-transcribed into cDNA using the mRNA RT Reagent Kit (RR047A; TaKaRa, Shiga, Japan). RT-PCR using FastStart Universal SYBR Green Master (ROX) (04913914001; Roche, Mannheim, Germany) was carried out on an Applied Biosystems 7500 real-time PCR system (Applied Biosystem, Foster City, CA, USA). The gene ACTIN served as an endogenous control for normalization. Primers used were as follows: *THBS3* forward primer, ATGGAGACGCAGGAAGCTTCG; *THBS3* reverse primer, AGGCTGTCCGATCTTCTCT; ACTIN forward primer, CATCCGCAAAGACCTGTACG; ACTIN reverse primer, CCTGCTTGCTGATCCACATC.

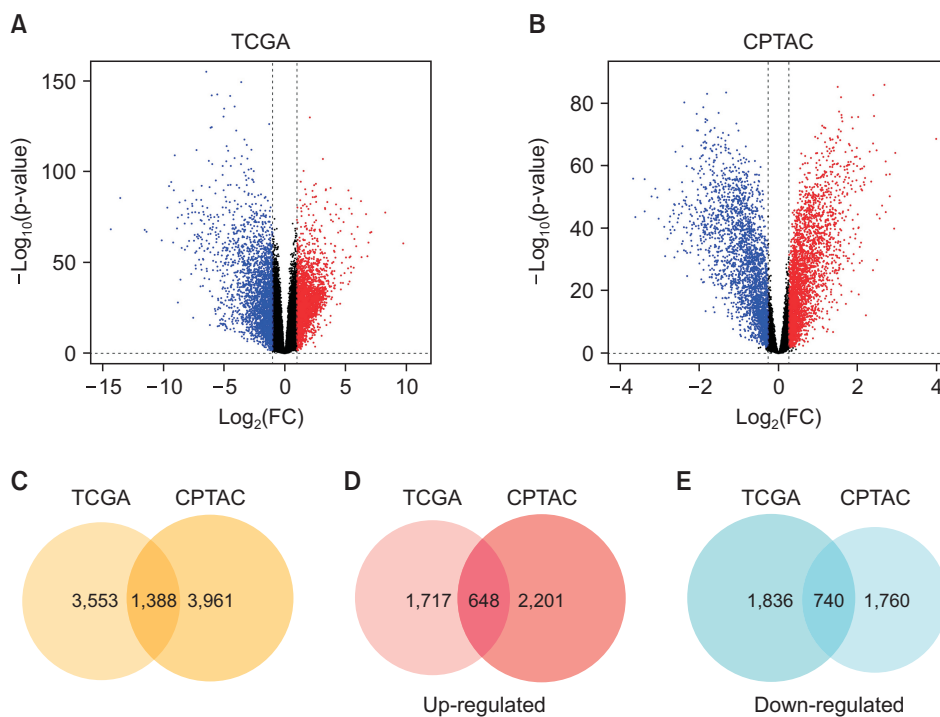


Fig. 1. Identification of differentially expressed genes and proteins. (A) Identified 4,941 DEGs in the ccRCC TCGA datasets. They are plotted in the volcano plot, in which the logarithmic ratios of the fold change (FC) of tumor/normal are plotted against negative logarithmic p-values. Of these 4,941 DEGs, 2,576 genes were significantly downregulated (blue), 2,365 genes were upregulated (red) ($|FC| > 2$, $p < 0.05$). (B) Identified 5,349 DEPs in the ccRCC CPTAC datasets, of which 2,500 proteins were downregulated and 2,849 proteins were upregulated ($|FC| > 1.2$, $p < 0.05$). (C) Analysis of the overlapping genes/proteins in the TCGA and CPTAC databases. Analysis of the overlapping (D) upregulated or (E) downregulated genes/proteins in the TCGA and CPTAC databases, respectively. DEG, differentially expressed gene; ccRCC, clear cell renal cell carcinoma; TCGA, The Cancer Genome Atlas; DEP, differentially expressed protein; CPTAC, Clinical Proteomic Tumor Analysis Consortium.

9. Database

The gene expression profiles and clinical data of patients were obtained from UCSC Xena (<https://xenabrowser.net/datapages/>) and the protein expression profiles were obtained from CPTAC (<https://proteomics.cancer.gov/programs/cptac>). The TIMER online tool was used to analyze the expression of the *THBS3* gene in different tumors (<http://timer.comp-genomics.org>).

comp-genomics.org).

10. Identification of differentially expressed genes and proteins

We identified DEGs in ccRCC from TCGA with $p < 0.05$ and $|\log_2\text{-fold change (FC)}| > 1$ and DEPs with $p < 0.01$ and $|\text{FC}| > 0.263$.

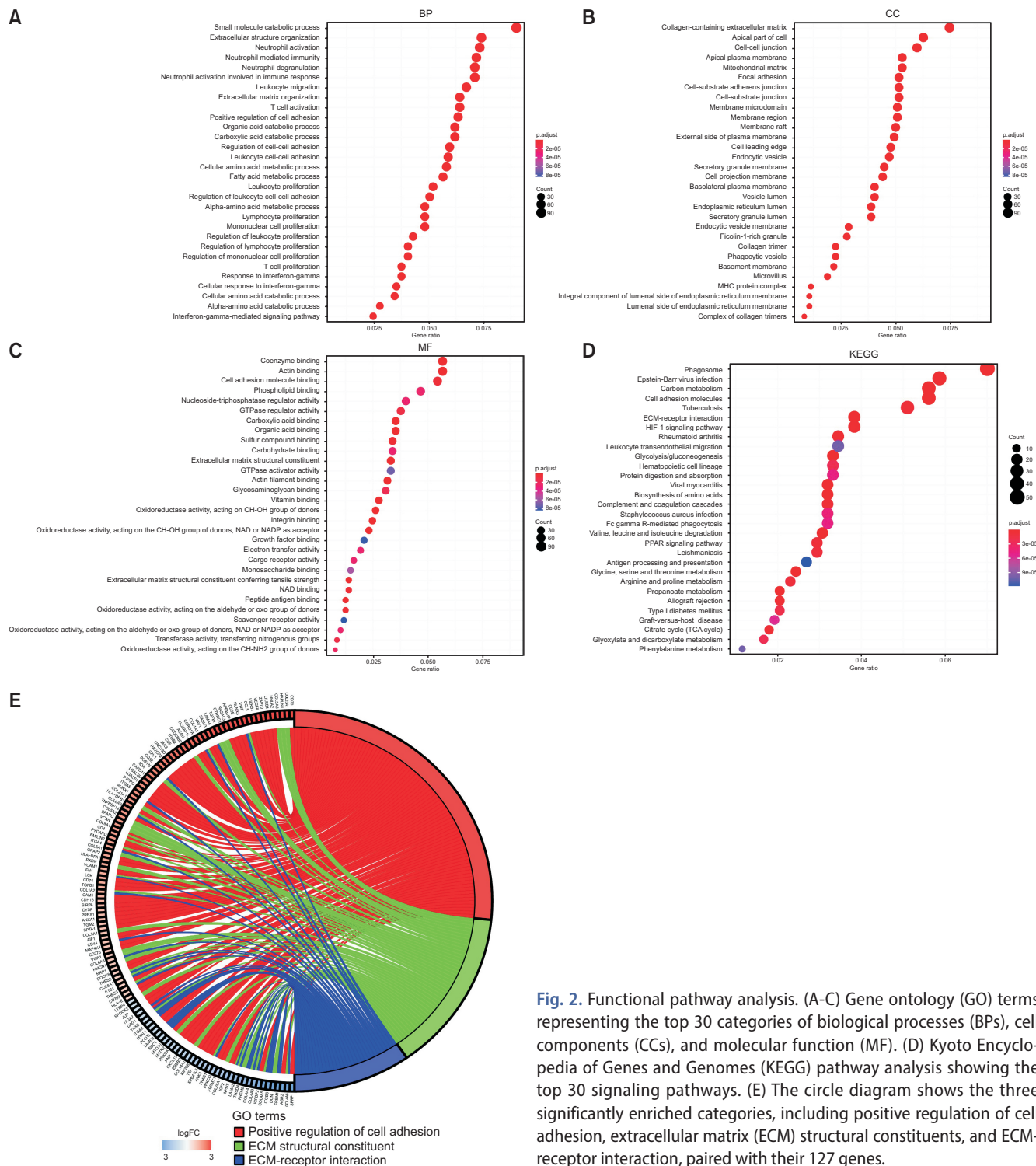


Fig. 2. Functional pathway analysis. (A-C) Gene ontology (GO) terms representing the top 30 categories of biological processes (BPs), cell components (CCs), and molecular function (MF). (D) Kyoto Encyclopedia of Genes and Genomes (KEGG) pathway analysis showing the top 30 signaling pathways. (E) The circle diagram shows the three significantly enriched categories, including positive regulation of cell adhesion, extracellular matrix (ECM) structural constituents, and ECM-receptor interaction, paired with their 127 genes.

11. Gene ontology (GO) and Kyoto Encyclopedia of Genes and Genomes (KEGG) pathway enrichment

We used the overlapping DEGs and DEPs for gene enrichment and functional annotation analysis by use of the “ClusterProfiler” package in R-3.6.1.

12. Overall survival, progression-free interval, and disease-specific survival analysis

The “Survival” R package was used to analyze the relationship between the expression level of 127 ECM and adhesion-associated genes and the overall survival (OS) of patients from the TCGA dataset. SPSS Statistics 24.0 software (IBM Corp., Armonk, NY, USA) was used to analyze the relationship between *THBS3* gene expression levels and OS, progression-free interval (PFI), and disease-specific survival (DSS). We tested this relationship by the Kaplan–Meier method with a log-rank test, where $p < 0.05$ was regarded as statistically significant.

13. Establishment of regression and overall survival risk prognostic models for clear cell renal cell carcinoma

After screening the ccRCC samples with complete clinical information, we used univariate Cox regression analyses to investigate the correlation between the expression of 16 survival-related DEGs and the OS of ccRCC patients. Subsequently, the correlation between genes and some clinical characteristics, including tumor dimension, histologic grade, pathologic M stage, and OS, were investigated by use

of multivariate analysis. Time-dependent receiver operating characteristic (ROC) curve analysis for OS was used to evaluate the accuracy of the prognostic model. An area under the curve (AUC) of 0.7 or greater was considered to be a significant predictive value.

14. Statistical analysis

All statistical analyses were performed using GraphPad Prism 8.0 (GraphPad Software, Inc, USA), SPSS Statistics 23.0 software, and R 3.6.1. The univariate and multivariate Cox hazard analysis of clinical characteristics was performed by using the “Survival” package, and time-dependent ROC curve analysis was performed by using the “survival-ROC” package. All *in vitro* experiments were performed in triplicate or quintuplicate and all data are represented as mean±standard deviation. A confidence threshold, $p < 0.05$, was used to analyze statistical significance as follows: * $p < 0.05$; ** $p < 0.01$; *** $p < 0.001$.

RESULTS

1. Comparative bioinformatics analysis of differentially expressed genes and proteins in clear cell renal cell carcinoma samples

The comparative study of DEGs and DEPs in ccRCC clinical samples was conducted in accordance with the scheme shown in Supplementary Fig. 1. The datasets for DEGs and DEPs in ccRCC clinical samples were extracted from the TCGA and CPTAC databases. Genes from the TCGA database were considered up- or downregulated be-

Table 1. Results of the univariate and multivariate Cox regression analyses of overall survival

Gene	Univariate analyses			Multivariate analyses		
	HR	95% CI	p-value	HR	95% CI	p-value
<i>ITGA8</i>	0.566	0.418–0.767	<0.001	0.670	0.469–0.958	0.028
<i>COL4A4</i>	0.561	0.413–0.763	<0.001	0.521	0.362–0.752	<0.001
<i>LGALS1</i>	1.792	1.321–2.432	<0.001	1.031	1.013–1.048	<0.001
<i>UNC13D</i>	1.597	1.182–2.157	0.002			
<i>RUNX1</i>	1.459	1.080–1.971	0.013			
<i>PODXL</i>	0.540	0.399–0.733	<0.001			
<i>THBS3</i>	2.458	1.797–3.362	<0.001	1.431	1.007–2.033	0.046
<i>COL6A1</i>	1.431	1.061–1.929	0.018	1.478	1.043–2.094	0.028
<i>FREM2</i>	0.689	0.510–0.931	0.014			
<i>PYCARD</i>	1.730	1.275–2.347	<0.001	1.516	1.059–2.171	0.023
<i>TEK</i>	0.500	0.367–0.680	<0.001			
<i>JAK3</i>	1.442	1.068–1.947	0.017			
<i>CCDC88B</i>	1.558	1.154–2.102	0.004			
<i>ANK3</i>	0.482	0.354–0.658	<0.001	0.522	0.363–0.750	<0.001

HR, hazard ratio; CI, confidence interval.

tween normal and tumor tissues when their absolute FC (tumor/normal) was larger than 2 ($FC > 2$) and their p-value was less than 0.05. Proteins from the CPTAC datasets were considered up- or downregulated when their absolute FC was larger than 1.2 ($FC > 1.2$) and their p-value was less than 0.01. These screening criteria resulted in the identification of 4,941 genes and 5,349 proteins as DEGs and DEPs, respectively, in ccRCC samples (Fig. 1A, B). The 1,388 overlapping DEG/DEPs were identified and are presented as a Venn diagram (Fig. 1C), of which 648 and 740 were found to be up- or downregulated, respectively (Fig. 1D, E). The complete lists of all genes, proteins, and genes/proteins contained in each Venn diagram intersection are included in Supplementary Table 1.

2. Identification of ECM-related and adhesion-associated genes

A total of 1,388 overlapping DEGs were used to perform functional enrichment analysis including GO and KEGG analysis in R 3.6.1. The top 30 enriched functions are shown in Fig. 2A-D, including biological processes, cell components, and molecular function. The results showed enrichment of many genes related to the ECM and adhesion. The circle diagram shows the significantly enriched categories, including positive regulation of cell adhesion, ECM structural constituents, and ECM-receptor interactions, with their 127 genes (Fig. 2E). A complete list of the 127 genes is included in Supplementary Table 2.

3. Identification of potential prognosis-related genes in clear cell renal cell carcinoma

The 127 DEGs linked to the ECM and cell adhesion were subjected to OS analysis using paired TCGA clinical datasets. The analysis revealed that 16 genes were significantly associated with the OS of ccRCC patients (Supplementary Fig. 2). The increased expression of 10 of these genes was correlated with a higher risk and the remaining 6 with lower risk for OS in ccRCC. Subsequently, univariate Cox regression analyses were performed to explore the relationship with gene expression by using the Kaplan–Meier survival package in R. Those genes with $p < 0.05$ were considered to correspond to prognosis-related candidate hubs, and 14 potential hubs were selected (Table 1). The clinicopathologic features of the patients are shown in Table 2. A total of 364 samples, including complete clinicopathologic data for all focus features, were selected for subsequent analysis. A multivariate Cox regression test (a collaborative correlation analysis between gene expression and clinical characteristics including tumor dimension, histologic grade, pathologic M stage, and OS) was

applied to the 14 selected hubs that were proposed to identify more reliable prognostic hubs (Table 1). Next, the prognostic value of a 7-gene prognostic signature was assessed by use of time-dependent ROC curve analysis (Table 1). Our results revealed that the AUCs of the 1-, 3-, and 5-year OS prediction scores for the significant gene *THBS3* were 0.759, 0.699, and 0.715, respectively (Fig. 3K). Thus, our systematic analysis indicated that *THBS3* is a reliable prognostic gene for ccRCC.

4. Association of high *THBS3* transcript levels with various clinicopathologic features and poor prognosis in clear cell renal cell carcinoma

The clinicopathologic features of the patients are shown in Table 2. The analyses of the ccRCC datasets in the CP-

Table 2. Clinical and pathologic features of the patients

Characteristic	Number of patients
TCGA datasets	
Tissue type	
Normal	72
Tumor	533
Pathologic stage	
I	172
II	32
III	93
IV	67
Pathologic M stage	
M0	300
M1	64
Histologic grade	
G1	5
G2	145
G3	150
G4	64
Tumor dimension	
< 1	201
≥ 1	163
Sex	
Male	242
Female	122
Pathologic N stage	
N0	172
N1	9
NX	183
CPTAC datasets	
Tissue type	
Normal	84
Tumor	110

TCGA, The Cancer Genome Atlas; CPTAC, Clinical Proteomic Tumor Analysis Consortium.

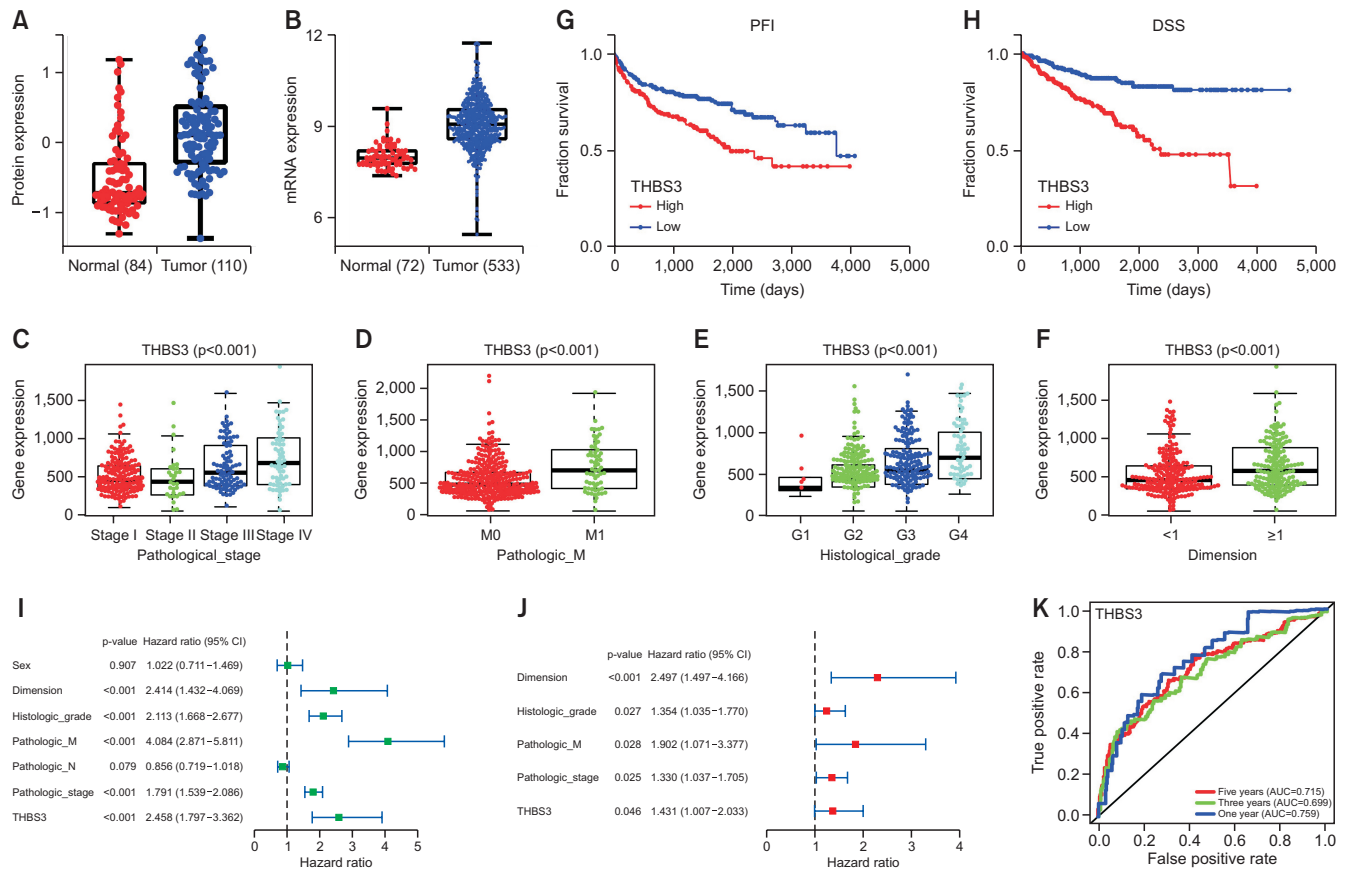


Fig. 3. Identification of *THBS3* overexpression is associated with poor prognosis of ccRCC. (A, B) *THBS3* protein and gene expression in ccRCC normal tissues and tumor tissues according to CPTAC and TCGA datasets. (C–F) *THBS3* expression was analyzed in ccRCC patients regarding pathologic stage, pathologic M grade, histologic grade, and dimension. (G, H) *THBS3* was upregulated in ccRCC patients and was related to a shorter PFI and DSS based on the TCGA dataset. (I, J) Univariate and multivariate Cox regression analyses of *THBS3* and some clinical characteristics for OS in ccRCC. (K) The time-dependent ROC curves for 1-, 3-, and 5-year OS predictions for the *THBS3* prognostic signature. ccRCC, clear cell renal cell carcinoma; CPTAC, Clinical Proteomic Tumor Analysis Consortium; TCGA, The Cancer Genome Atlas; PFI, progression-free interval; DSS, disease-specific survival; OS, overall survival; ROC, receiver operating characteristic; AUC, area under the curve.

TAC and TCGA showed expression levels of the *THBS3* protein (Fig. 3A) and gene (Fig. 3B) to be significantly upregulated in the tumor tissues of ccRCC patients. We also investigated the gene expression of *THBS3* in other cancers. Our analyses revealed that *THBS3* was not only overexpressed in ccRCC tumor samples but also in other cancer samples, such as cholangiocarcinoma, pancreatic adenocarcinoma, and stomach adenocarcinomas (Supplementary Fig. 3C). Analysis of the TCGA dataset revealed that *THBS3* was highly expressed in the tissues of patients with advanced tumor pathologic stages, distant metastasis, higher tumor histologic grades, and large tumor size (Fig. 3C–F). Further, OS was significantly worse in the ccRCC patients with high *THBS3* expression than in those with low *THBS3* gene expression (Supplementary Fig. 2A), similar to the relation observed for the PFI (Fig. 3G) and DSS (Fig. 3H). Univariate Cox regression analysis was performed to select the related variables for multivariate Cox analysis (Fig. 3I). The multivariate Cox

analysis showed that high *THBS3* expression was an independent prognostic factor for OS (Fig. 3J). Time-dependent ROC curve analysis further confirmed the diagnostic value of *THBS3* expression in ccRCC progression (Fig. 3K).

5. Repression of proliferation and migration upon downregulation of *THBS3* in clear cell renal cell carcinoma cells

To assess the effect of silencing the expression of *THBS3* on the proliferation and migration of ccRCC cells, *THBS3* expression was downregulated in ACHN and 769-P cells after transfection with specific siRNAs. This RT-PCR further confirmed that mRNA expression was significantly downregulated in the siRNA-transfected cells compared with the mock-transfected cells (Supplementary Fig. 3A, B). Subsequent CCK8 assays with these cells indicated that *THBS3* knockdown results in significant suppression of cell proliferation of ccRCC cells compared with negative control

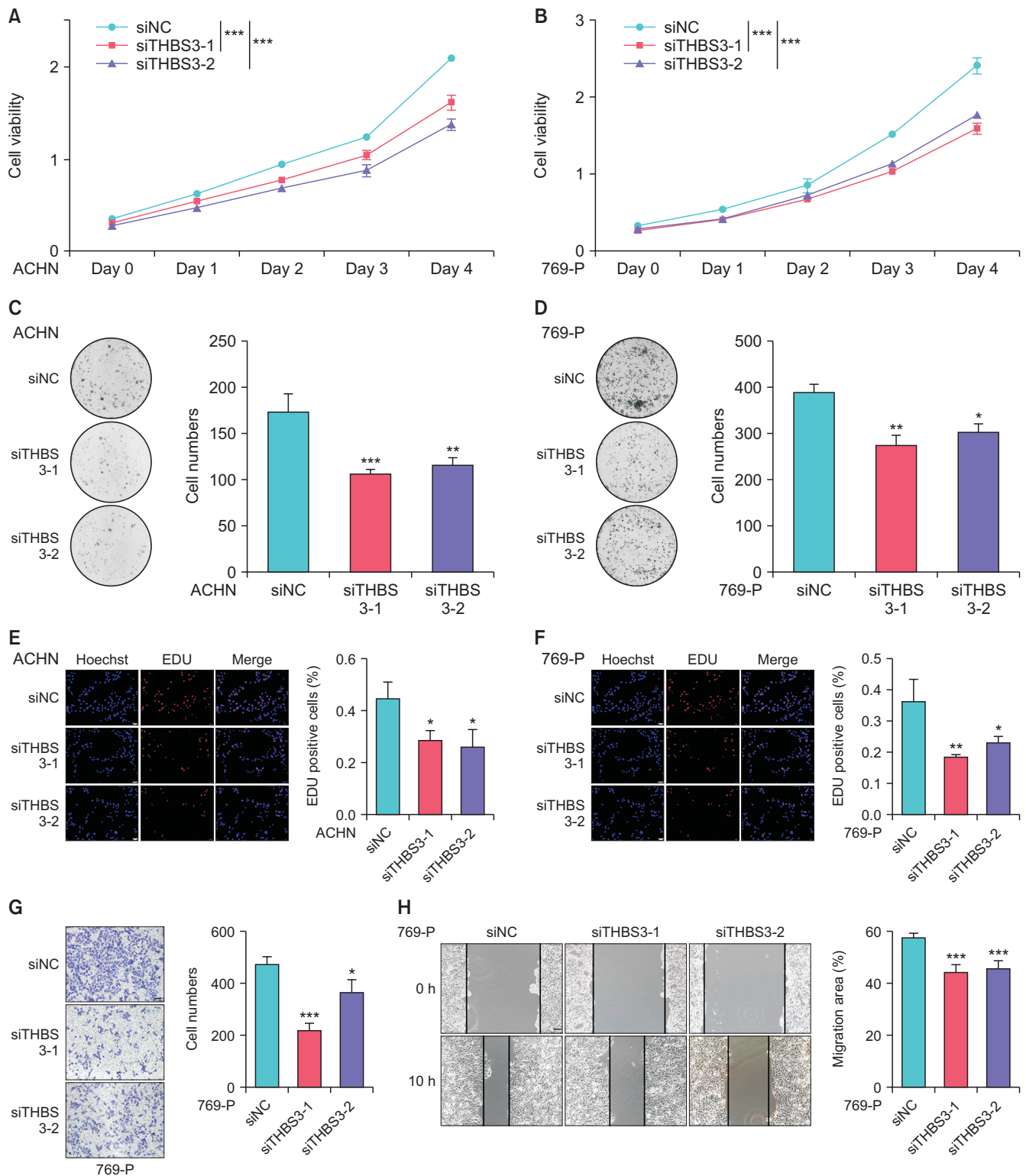


Fig. 4. Depletion of *THBS3* suppresses ccRCC growth and metastasis. (A, B) CCK8 assay of ACHN and 769-P cells transfected with *THBS3* siRNA or control siRNA. The proliferation rates of cells transfected with *siTHBS3* were significantly lower than those of the control cells. (C, D) *THBS3* knockdown significantly suppressed colony formation. The use of crystal violet for dyeing has been described in the section of materials and methods (Colony formation assay). The every hole in the 6-well plates is the original image taken directly from a high-resolution mobile phone in black and white mode and using manual counting. (E, F) EDU assays were performed to assess cell viability and proliferation. Scale bar: 50 μ m. (G, H) Transwell assays and wound healing were used to evaluate cell migration ability. Scale bar: 100 μ m. All values are expressed as the mean \pm standard deviation (* p <0.05, ** p <0.01, *** p <0.001). ccRCC, clear cell renal cell carcinoma.

(Fig. 4A, B). Moreover, significantly fewer colonies were formed when *THBS3* was silenced in ccRCC cells than in respective mock-transfected cells (Fig. 4C, D). An EDU assay showed that the number of red fluorescent cells indicative of DNA synthesis during proliferation decreased in the si*THBS3*-1 and si*THBS3*-2 groups in ACHN and 769-P cells (Fig. 4E, F). Next, the migratory ability of ccRCC cells was tested in *THBS3* knockdown cells. The results showed that knockdown of *THBS3* significantly inhibited the migration of 769-P cells compared with mock-transfected cells (Fig. 4G). Furthermore, wound-healing assays demonstrated that *THBS3* suppression considerably attenuated the migratory capacity of ccRCC cells (Fig. 4H). Overall, the above results confirm that *THBS3* has a critical effect on the proliferation and migration of ccRCC cells.

DISCUSSION

Nearly 75% of RCC cases are ccRCC, which is characterized by clear or occasionally eosinophilic granularity of the cancer cells. ccRCC is one of the deadliest renal tumors worldwide [1,2]. Early screening of ccRCC markers is limited, as is the accuracy of these markers. The tumorigenesis of ccRCC is known to involve many molecular events, such as ECM and adhesion. Scelo et al. [19] found novel pathways and genes affected by recurrent mutations and abnormal transcriptome patterns, including focal adhesion and components of the ECM, by constructing a genomic landscape across Europe. Ho et al. [20] have revealed the upregulation of ECM genes through differential gene expression profiling of matched primary RCCs and metastases. The ECM pathway has been shown to have an important role in tumor progression and is regarded as a therapeutic target in cancer [21]. For instance, collagen 1 [22] and PDE7B [23], which are involved in ECM pathways, play a key role in the development of metastatic RCC. In addition, ECM-related genes have shown promising insights for exploring novel prognostic biomarkers for ccRCC. High-throughput sequencing technology has facilitated the detection of promising hubs related to the prognosis and treatment of ccRCC. In this study, we used TCGA and CPTAC databases to screen for genes and proteins related to the ECM and cell adhesion to explore novel prognostic biomarkers and therapeutic targets of ccRCC. Among the 16 ECM-related genes identified in bioinformatics analyses, *JAK3* [24], *TEK* [25], *ITGA8* [26], and *RUNX1* [27] have been reported as markers for predicting the prognosis of ccRCC.

In our study, *THBS3* emerged as a reliable prognostic gene for ccRCC. We demonstrated that the expression of

THBS3, a gene associated with the ECM and adhesion, is significantly upregulated in ccRCC tumors and that elevated expression of *THBS3* is associated with poor clinical outcomes, such as tumor stage, tumor dimension, tumor metastasis, and survival status of patients. Kaplan–Meier curves of OS, PFI, and DSS demonstrated that high *THBS3* expression is remarkably associated with worse survival status in patients. The results of univariate and multivariate analysis indicated that upregulated *THBS3* predicted a higher risk of death, and time-dependent ROC curve analyses further confirmed its prognostic capability. Thus, our studies suggested that *THBS3* is sufficient for use as a prognostic biomarker.

Two other studies have proved an elevated level of *THBS3* in osteosarcoma [16] and chronic myeloid leukemia [28], respectively. In our study, *THBS3* was also found to be upregulated in many other solid tumors, such as in pancreatic adenocarcinoma and stomach adenocarcinomas, suggesting that *THBS3* might be a critical molecular target in human cancers. We also demonstrated that *THBS3* expression is significantly upregulated in ccRCC tumor tissues compared with adjacent normal tissues. Moreover, downregulation of *THBS3* in ACHN and 769-P suppresses their malignant phenotype, indicating that *THBS3* likely promotes tumor progression in ccRCC. *THBS3* is a cell matrix protein that functions as an adhesion molecule [11]. In fact, there is no coverage of the role of *THBS3* in the progression of ccRCC. Our study suggests the potential for use of *THBS3* as a therapeutic target.

Our study has a few limitations. The main limitation of our findings is that we used public databases, and thus our findings need to be validated in prospective clinical trials. The functions of *THBS3* that impact the development and progression of ccRCC need to be further investigated *in vivo*. In summary, our findings suggest that *THBS3* could serve as a potential prognostic and therapeutic target in ccRCC, and further research is needed to explore the relevant molecular pathways of *THBS3* in ccRCC.

CONCLUSIONS

We revealed that *THBS3* is upregulated in ccRCC cancer tissues. It could be used as a novel prognostic marker for ccRCC. Our findings offer theoretical support to study ECM and adhesion proteins in ccRCC, which may provide a new perspective for the clinical management of ccRCC.

CONFLICTS OF INTEREST

The authors have nothing to disclose.

ACKNOWLEDGMENTS

This research was supported by the China Postdoctoral Science Foundation (2019M663098), by the National Natural Science Foundation of China (81772736, 81972366), the Guangdong Key Laboratory funds of Systems Biology and Synthetic Biology for Urogenital Tumors (2017B030301015), the Basic Research Project of Shenzhen Science and Technology Plan (20190726095103499), and by Shenzhen Science and Technology Innovation Commission (JSGG20191231141403880).

AUTHORS' CONTRIBUTIONS

Research conception and supervising: Aifa Tang. Bioinformatics data analysis, CCK8, colony formation, EDU assays execution, original draft writing: Xiangling Chen and Jiantian Lin. Wound-healing and invasion execution: Min Chen. Drafting discussion of manuscript: Qiaoling Chen. Guidance on data collection and revising the article: Zhiming Cai.

SUPPLEMENTARY MATERIALS

Supplementary materials can be found via <https://doi.org/10.4111/icu.20210273>.

REFERENCES

1. Hsieh JJ, Purdue MP, Signoretti S, Swanton C, Albiges L, Schmidinger M, et al. Renal cell carcinoma. *Nat Rev Dis Primers* 2017;3:17009.
2. Capitanio U, Bensalah K, Bex A, Boorjian SA, Bray F, Coleman J, et al. Epidemiology of renal cell carcinoma. *Eur Urol* 2019;75:74-84.
3. Zisman A, Pantuck AJ, Wieder J, Chao DH, Dorey F, Said JW, et al. Risk group assessment and clinical outcome algorithm to predict the natural history of patients with surgically resected renal cell carcinoma. *J Clin Oncol* 2002;20:4559-66.
4. Powles T, Staehler M, Ljungberg B, Bensalah K, Canfield SE, Dabestani S, et al. European Association of Urology guidelines for clear cell renal cancers that are resistant to vascular endothelial growth factor receptor-targeted therapy. *Eur Urol* 2016;70:705-6.
5. Diamond E, Molina AM, Carbonaro M, Akhtar NH, Giannakakou P, Tagawa ST, et al. Cytotoxic chemotherapy in the treatment of advanced renal cell carcinoma in the era of targeted therapy. *Crit Rev Oncol Hematol* 2015;96:518-26.
6. Liu X, Simon JM, Xie H, Hu L, Wang J, Zurlo G, et al. Genome-wide screening identifies SFMBT1 as an oncogenic driver in cancer with VHL loss. *Mol Cell* 2020;77:1294-306.e5.
7. Schrödter S, Braun M, Syring I, Klümper N, Deng M, Schmidt D, et al. Identification of the dopamine transporter SLC6A3 as a biomarker for patients with renal cell carcinoma. *Mol Cancer* 2016;15:10.
8. Wang M, Li X, Zhang J, Yang Q, Chen W, Jin W, et al. AHN-AK2 is a novel prognostic marker and oncogenic protein for clear cell renal cell carcinoma. *Theranostics* 2017;7:1100-13.
9. Romani P, Valcarcel-Jimenez L, Frezza C, Dupont S. Crosstalk between mechanotransduction and metabolism. *Nat Rev Mol Cell Biol* 2021;22:22-38.
10. Mishra YG, Manavathi B. Focal adhesion dynamics in cellular function and disease. *Cell Signal* 2021;85:110046.
11. Vos HL, Devarayalu S, de Vries Y, Bornstein P. Thrombospondin 3 (Thbs3), a new member of the thrombospondin gene family. *J Biol Chem* 1992;267:12192-6.
12. Stenina-Adognravi O. Thrombospondins: old players, new games. *Curr Opin Lipidol* 2013;24:401-9.
13. Schips TG, Vanhoutte D, Vo A, Correll RN, Brody MJ, Khalil H, et al. Thrombospondin-3 augments injury-induced cardiomyopathy by intracellular integrin inhibition and sarcolemmal instability. *Nat Commun* 2019;10:76.
14. Bergmeier V, Etich J, Pitzler L, Frie C, Koch M, Fischer M, et al. Identification of a myofibroblast-specific expression signature in skin wounds. *Matrix Biol* 2018;65:59-74.
15. Hankenson KD, Hormuzdi SG, Meganck JA, Bornstein P. Mice with a disruption of the thrombospondin 3 gene differ in geometric and biomechanical properties of bone and have accelerated development of the femoral head. *Mol Cell Biol* 2005;25:5599-606.
16. Dalla-Torre CA, Yoshimoto M, Lee CH, Joshua AM, de Toledo SR, Petrilli AS, et al. Effects of THBS3, SPARC and SPP1 expression on biological behavior and survival in patients with osteosarcoma. *BMC Cancer* 2006;6:237.
17. Adolph KW. Relative abundance of thrombospondin 2 and thrombospondin 3 mRNAs in human tissues. *Biochem Biophys Res Commun* 1999;258:792-6.
18. Ren Y, Wang Y, Hao S, Yang Y, Xiong W, Qiu L, et al. NFE2L3 promotes malignant behavior and EMT of human hepatocellular carcinoma (HepG2) cells via Wnt/ β -catenin pathway. *J Cancer* 2020;11:6939-49.
19. Scelo G, Riazalhosseini Y, Greger L, Letourneau L, González-Porta M, Wozniak MB, et al. Variation in genomic landscape of clear cell renal cell carcinoma across Europe. *Nat Commun* 2014;5:5135.
20. Ho TH, Serie DJ, Parasramka M, Cheville JC, Bot BM, Tan W, et al. Differential gene expression profiling of matched primary renal cell carcinoma and metastases reveals upregulation of extracellular matrix genes. *Ann Oncol* 2017;28:604-10.

21. Järveläinen H, Sainio A, Koulu M, Wight TN, Penttinen R. Extracellular matrix molecules: potential targets in pharmacotherapy. *Pharmacol Rev* 2009;61:198-223.
22. Majo S, Courtois S, Souleyreau W, Bikfalvi A, Auguste P. Impact of extracellular matrix components to renal cell carcinoma behavior. *Front Oncol* 2020;10:625.
23. Sun Y, Zou J, Ouyang W, Chen K. Identification of *PDE7B* as a potential core gene involved in the metastasis of clear cell renal cell carcinoma. *Cancer Manag Res* 2020;12:5701-12.
24. de Martino M, Gigante M, Cormio L, Prattichizzo C, Cavalcanti E, Gigante M, et al. JAK3 in clear cell renal cell carcinoma: mutational screening and clinical implications. *Urol Oncol* 2013;31:930-7.
25. Ha M, Son YR, Kim J, Park SM, Hong CM, Choi D, et al. TEK is a novel prognostic marker for clear cell renal cell carcinoma. *Eur Rev Med Pharmacol Sci* 2019;23:1451-8.
26. Lu X, Wan F, Zhang H, Shi G, Ye D. ITGA2B and ITGA8 are predictive of prognosis in clear cell renal cell carcinoma patients. *Tumour Biol* 2016;37:253-62.
27. Rooney N, Mason SM, McDonald L, Däbritz JHM, Campbell KJ, Hedley A, et al. RUNX1 is a driver of renal cell carcinoma correlating with clinical outcome. *Cancer Res* 2020;80:2325-39.
28. Simanovsky M, Berlinsky S, Sinai P, Leiba M, Nagler A, Galski H. Phenotypic and gene expression diversity of malignant cells in human blast crisis chronic myeloid leukemia. *Differentiation* 2008;76:908-22.